Two-quasiparticle states in the interacting boson model. II. Electromagnetic properties in the SU(3) limit

D. Vretenar and V. Paar
Department of Physics, Faculty of Science, University of Zagreb, 41000 Zagreb, Republic of Croatia, Yugoslavia

M. Savoia and G. Bonsignori
Istituto Nazionale di Fisica Nucleare, Sezione di Bologna, Bologna, Italy and Department of Physics "A. Righi", Via Irnerio 46, Bologna, Italy

(Received 18 March 1991)

The interacting boson approximation model, extended by allowing one boson to break and form a quasiparticle pair, is investigated in the SU(3) limit. Electromagnetic properties of yrast states are studied for the algebraic analogs of both the decoupling and strong-coupling limits. The effects of a pair-breaking interaction that mixes states with different numbers of quasiparticles are investigated for $E2$ transitions between yrast states. For the algebraic analog of the decoupling limit, it is shown that the mixing interaction has a strong influence on transitions in the region of crossing between the ground-state band and the lowest two-quasiparticle (2qp) band. The mixing interaction does not change the electromagnetic properties of the states of the ground-state band. This effect is due to the approximate cancellation between self-energy and vertex corrections, which corresponds to the nuclear Ward identity. For the algebraic analog of the strong-coupling limit, the K forbiddeness of $E2$ transitions between the ground-state band and the lowest 2qp band is high, and therefore the influence of the mixing interaction is negligible.

I. INTRODUCTION

The physics of high-spin states in nuclei has been traditionally described in the framework of models that are based on the cranking approximation [cranking Nilsson model, cranking Hartree-Fock-Bogoliubov (HFB) scheme]. During the last decade, however, there have also been attempts to describe two-quasiparticle high-spin states in even-even nuclei within the framework of the interacting boson model (IBM) [1]. The model, which has been used mostly in the description of low-spin states, can be extended to high-spin physics by including more and more of the original shell model space through the breaking of the correlated S and D pairs. High-spin states are therefore described in terms of broken pairs. Various extensions of the IBM have been reported [2–6] that include selective noncollective two-fermion states in addition to bosons. Gelberg and Zemel [2] used an empirical model to incorporate two-particle states in an SU(3) boson basis and investigated the backbending phenomenon in the region of band crossing. Faessler *et al.* [3] have proposed a semimicroscopic model for the inclusion of two-quasiparticle states in a boson basis. The model is based on the IBM-1, and the boson-fermion interactions are derived in analogy to the interacting boson-fermion model [21]. The model has been successfully applied to the description of high-spin states and their electromagnetic properties in Hg, Ba and Ce isotopes. Yoshida *et al.* [4] extended the neutron-proton IBM (IBM-2) to include a pair of nucleons. The model has been applied to the description of Ge [4] and Dy [5] isotopes. Chuu, Hsieh, and Chiang used the interacting boson approximation plus one-fermion-pair model to investigate the structure of high-spin states in Pt and Dy isotopes [6]. Recently, we have further extended the IBM to include two- and four-fermion noncollective states (one and two broken pairs) [7,8]. Our model is based on the IBM-1, i.e., the boson space consists of s and d bosons only, and no distinction between protons and neutrons is made. A boson can break to form a noncollective fermion pair. The one and two broken pairs are represented by two- and four-quasiparticle states, respectively. All calculations are performed in the laboratory frame, and therefore they produce results that can be directly compared to experimental data, in contrast to the cranking model calculations. One straightforward application of the model is the description of backbending phenomena in deformed nuclei [crossings between rotational bands, behavior of the moment of inertia as function of angular momentum, two-quasiparticle (2qp) admixtures in the ground-state band, reduction of $B(E2)$ values in the region of crossing, etc.]. In Ref. [7], which will be referred to as paper I, we have investigated the formation of band patterns based on two- and four-quasiparticle states in the SU(3) limit of the model. In both the strong-coupling and decoupling limits we have derived algebraic bases that allow the classification of low-lying 2qp bands. We have also studied the behavior of the moment of inertia as function of angular velocity.

In the present work we will continue our investigation of the SU(3) limit of the model and, in particular, will study the electromagnetic properties of yrast states. In the last few years data on electromagnetic transition rates, static moments, and g factors for high-spin states have been measured in many nuclei. Up to now most of

these data have not been explained satisfactorily, and there are also many experimental uncertainties. Therefore, we feel that a general theoretical investigation might elucidate some typical points. For simplicity, in the present paper we consider only yrast states: the ground-state band and the yrast 2qp band. Experimental data on electromagnetic properties are mostly known for yrast states, and the general properties of side bands close to the yrast line are similar to those of the lowest band. A common feature in our results will be the presence of truncation effects. These are caused by the truncation of the model space (finite number of bosons), which restricts the values of the core angular momentum. Truncation effects appear in all nuclear models that are based on finite configuration spaces. In order to reduce truncation effects, we have increased the number of bosons N, as compared to the examples that were studied in paper I. This is the reason why we have not been able to include four-quasiparticle states in the present calculations—the bases would have been enormous. In Sec. II we investigate the electromagnetic properties of yrast states in the decoupling limit. In this limit particle-type (hole-type) fermions are coupled to the SU(3) prolate (oblate) core. The boson-fermion interaction is repulsive for the lowest 2qp states and the low-lying bands are decoupled. An interesting result is that the pair-breaking interaction, which mixes states with different number of quasiparticles, practically does not affect the $B(E2)$ values for transitions within the ground-state band. In Sec. III this effect is discussed in the framework of nuclear Ward identities. In Sec. IV we present $B(E2)$ values, static moments, and g factors of yrast states for the case of hole-type (particle-type) fermions coupled to the SU(3) prolate (oblate) core—the strong coupling limit.

II. DECOUPLING LIMIT

We will start with an illustrative calculation for the model case similar to the one described in paper I: a prolate boson core characterized by SU(3) symmetry and the fermion space is restricted to the unique-parity orbital $h\frac{11}{2}$. Although, in general, the fermions occupy all the single-particle orbitals from which the bosons have been mapped, for the description of $\pi=+1$ 2qp states close to the yrast line the most important are the unique-parity high-j orbitals ($g\frac{9}{2}$, $h\frac{11}{2}$, $i\frac{13}{2}$). The Hamiltonian of the system is [7]

$$H=\sum_{\alpha}E_{\alpha}a_{\alpha}^{\dagger}\tilde{a}_{\alpha}+H_B+H_{\mathrm{DYN}}+V_{\mathrm{MIXING}} \ . \tag{1}$$

The first term is the single-quasiparticle Hamiltonian. H_B is the IBM-1 boson Hamiltonian in the SU(3) limit [1]:

$$H_B=-\alpha\hat{Q}_B^{(2)}\cdot\hat{Q}_B^{(2)}+\beta\hat{I}_B^{(1)}\cdot\hat{I}_B^{(1)} \ , \tag{2}$$

where $Q_B^{(2)}$ is the boson quadrupole operator

$$\hat{Q}_B^{(2)}=d_{\mu}^{\dagger}\times s+s^{\dagger}\times\tilde{d}_{\mu}\pm\frac{\sqrt{7}}{2}(d^{\dagger}\times\tilde{d})^{(2)} \tag{3}$$

and

$$\hat{I}_B^{(1)}=\sqrt{10}(d^{\dagger}\times\tilde{d})^{(1)} \tag{4}$$

is the angular momentum operator. The dynamical term represents the long-range quadrupole-quadrupole interaction between the unpaired fermions and the boson core

$$H_{\mathrm{dyn}}=\Gamma_0\sum_j(u_j^2-v_j^2)\langle j\|Y_2\|j\rangle(a_j^{\dagger}\times\tilde{a}_j)^{(2)}\cdot\hat{Q}_B^{(2)} \ . \tag{5}$$

V_{MIXING} is the pair-breaking interaction that mixes states with different number of quasiparticles [7]:

$$V_{\mathrm{mixing}}=-u_2\sum_j 2u_jv_j\langle j\|Y_2\|j\rangle(a_j^{\dagger}\times a_j^{\dagger})^{(2)}\cdot\tilde{d}+\mathrm{H.c.} \tag{6}$$

This form is similar to the mixing interaction that was used by Faessler *et al.* [3]. H_{dyn} and V_{mixing} determine the basic structure of the energy spectrum. In the present calculation we have neglected the perturbations caused by the boson-fermion exchange interaction [7], and by the mixing interaction of rank zero in the fermion and boson parts [3,8]. Another term that has not been included in the Hamiltonian (1) is the residual fermion-fermion interaction (for example, a delta force). For a model description of unique parity states close to the yrast line such an interaction does not give an important contribution. Finally, the Hamiltonian (1) is diagonalized in the Hilbert space

$$|N \text{ bosons}\rangle\oplus|(N-1) \text{ bosons}\otimes 1 \text{ broken pair}\rangle \ . \tag{7}$$

The energy spectrum shown in Fig. 1 is calculated for

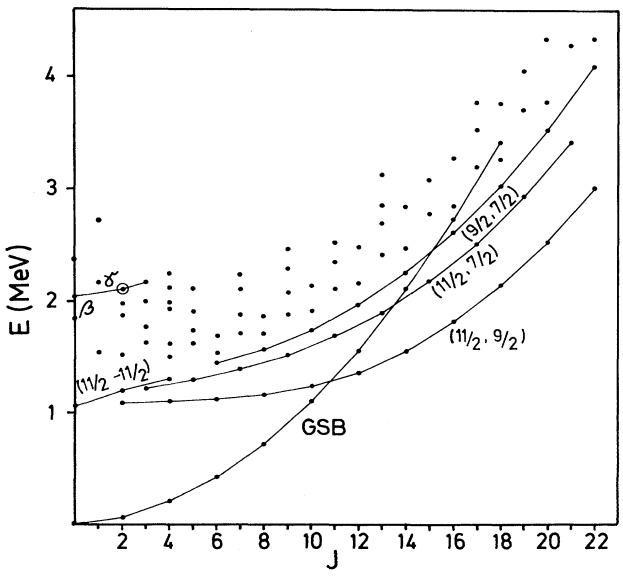

FIG. 1. Excitation energy versus angular momentum for the illustrative calculation in the decoupling limit: prolate SU(3) core with nine bosons, $h\frac{11}{2}$ orbital with $v^2=0.2$ and $E_{11/2}=0.85$ MeV; dynamical boson-fermion interaction with $\Gamma_0=0.45$ MeV; no mixing between states with different numbers of quasiparticles.

the first set of parameters, which will be referred to as parametrization (A):$\alpha=0.04$ MeV, $\beta=-0.005$ MeV, the number of bosons $N=9$; $h_{\frac{11}{2}}$ orbital with $v^2=0.2$ and $E_{11/2}=0.85$ MeV; dynamical boson-fermion interaction with $\Gamma_0=0.45$ MeV. In the parametrization (A) we take $u_2=0$, i.e., there is no mixing between states with different number of quasiparticles. Only the first few calculated levels of each angular momentum J are shown in the figure. The structure of the lowest 2qp bands depends on the position of the Fermi level. For particle-type (hole-type) fermions coupled to the SU(3) prolate (oblate) core, the dynamical boson-fermion interaction is repulsive for the lowest 2qp states, and the resulting spectrum is of decoupled type. 2qp states are organized into decoupled rotational bands with $\Delta J=2$ between neighboring states. These bands are characterized by the signature quantum number: $r=+1$ (-1) for states with even (odd) spin. The equivalent situation in the geometrical model of Bohr and Mottelson [9] arises when the unpaired fermions are decoupled from the deformation and, under the action of the Coriolis force, tend to align their angular momenta along the axis of rotation [10]. The lowest 2qp bands in Fig. 1 can be characterized to a good approximation by "algebraic projections" (α_1,α_2) [7]. In the geometrical limit when the number of bosons $N\rightarrow\infty$, the quantum numbers α_1 and α_2 correspond to the projections of the fermion angular momenta j_1 and j_2 on the axis of rotation. The lowest band is the most aligned: $(\alpha_1=j,\ \alpha_2=j-1)=(\frac{11}{2},\frac{9}{2})$. We have also identified two other bands: $(\alpha_1=j,\ \alpha_2=j-2)=(\frac{11}{2},\frac{7}{2})$ and $(\alpha_1=j-1,\ \alpha_2=j-2)=(\frac{9}{2},\frac{7}{2})$. For higher states the Coriolis mixing is much stronger and the classification into rotational bands becomes more difficult. If one plots the moment of inertia as a function of angular velocity for the yrast states, it is seen that the backbending of the moment of inertia is very pronounced at the crossing between the ground-state band and the 2qp band $(\frac{11}{2},\frac{9}{2})$ [7].

Let us now investigate the electromagnetic properties of the yrast states. The operators are defined in analogy with those that were derived in the semimicroscopic model by Faessler *et al.* [3]. The $E2$ operator is taken in the form

$$T(E2)=\frac{3}{4\pi}e^{\text{vib}}R_0^2[(d^\dagger\times\tilde{s}+s^\dagger\times\tilde{d})^{(2)}+\chi(d^\dagger\times\tilde{d})^{(2)}]$$
$$-e\frac{1}{\sqrt{5}}\sum_{j_1j_2}q_{j_1j_2}\{(u_{j_1}u_{j_2}-v_{j_1}v_{j_2})(a_{j_1}^\dagger\times\tilde{a}_{j_2})^{(2)}-\frac{u_{j_1}v_{j_2}}{\sqrt{N}}[(a_{j_1}^+\times a_{j_2}^+)^{(2)}\times\tilde{s}]^{(2)}+\frac{u_{j_2}v_{j_1}}{\sqrt{N}}[(\tilde{a}_{j_1}\times\tilde{a}_{j_2})^{(2)}\times s^\dagger]^{(2)}\}\ , \quad (8)$$

where

$$q_{j_1j_2}=\langle j_1\|r^2Y_2\|j_2\rangle\ . \quad (9)$$

We take $\langle r^2\rangle=\frac{3}{5}R_0^2$, and $R_0=0.12A^{1/3}\times10^{-12}$ cm. N is the number of bosons. The $M1$ operator is defined as

$$T(M1)=\sqrt{30/4\pi}\,g_R(d^\dagger\times\tilde{d})^{(1)}$$
$$-\frac{1}{\sqrt{4\pi}}\sum_{j_1j_2}[g_l\langle j_1\|\vec{j}\|j_2\rangle+(g_s-g_l)\langle j_1\|\vec{s}\|j_2\rangle]$$
$$\times\{(u_{j_1}u_{j_2}+v_{j_1}v_{j_2})(a_{j_1}^\dagger\times\tilde{a}_{j_2})^{(1)}-\frac{u_{j_1}v_{j_2}}{\sqrt{N}}[(a_{j_1}^\dagger\times a_{j_2}^\dagger)^{(1)}\times\tilde{s}]^{(1)}+\frac{u_{j_2}v_{j_1}}{\sqrt{N}}[(\tilde{a}_{j_1}\times\tilde{a}_{j_2})^{(1)}\times s^\dagger]^{(1)}\}\ . \quad (10)$$

In the calculation of electromagnetic properties we employ the following values for effective charges and gyromagnetic ratios: $e^{\text{vib}}=1.0$, $e=0.5$, $g_S=-2.678=0.7g_S^{\text{free}}(\nu)$, $g_l=0$, $g_R=0.4$. The nuclear radius R_0 is taken for an $A=100$ nucleus. In Fig. 2 we present the $B(E2)$ values for transitions between the yrast states from Fig. 1 (solid line). The dashed line connects the $B(E2)$'s for transitions within the ground-state band after the crossing with the 2qp band $(\frac{11}{2},\frac{9}{2})$. The gradual decrease of the $B(E2)$'s within the ground-state band (GSB) is due to the truncation of the boson space. Since there is no mixing between the GSB and the $(\frac{11}{2},\frac{9}{2})$ band, $(u_2=0)$, the transition between the bands is very weak: $B(E2,12_1\rightarrow10_1)=4.5\times10^{-3}\ e^2\text{fm}^4$. This contribution comes from the terms in the $E2$ operator (8) that do not conserve separately the number of fermions and the number of bosons, but only the total number of valence nucleons. The calculated electric quadrupole moments of the yrast states are shown in Fig. 3. We note the discontinuity at the intersection between the GSB and the $(\frac{11}{2},\frac{9}{2})$ 2qp band. In the SU(3) limit, the intrinsic quadrupole moment of the core is [11]

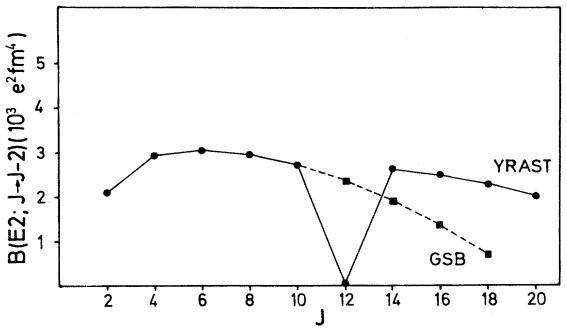

FIG. 2. $B(E2)$ values for transitions between the yrast states from Fig. 1 (solid line). The dashed line connects the $B(E2)$'s for transitions within the ground-state band. For a description of parameters, see the text.

$$Q_0=\pm\tfrac{3}{4}e^{\mathrm{VIB}}R_0^2(4N+3)\left[\frac{2}{5\pi}\right]^{1/2}, \tag{11}$$

where the sign + (−) corresponds to a prolate (oblate) core. For the parametrization that we have used, the intrinsic quadrupole moment is $Q_0=3.24$ $e\,b$. In the geometrical model [9] this corresponds to the deformation $\beta\approx 0.34$ (for a $Z=40$ nucleus). In Fig. 4 we display the g-factors of the yrast states. Again, since there is no mixing of the GSB with 2qp states, the g factors in the GSB have the constant value $g_R=0.4$. As the 2qp neutron band $(\frac{11}{2},\frac{9}{2})$ becomes the yrast band, the g factors change sign: $g(12_1)=-0.02$. With increasing angular momentum in this band, we note a steady increase of the g factors. In Fig. 4 we have also compared the g factors of the yrast band $(\frac{11}{2},\frac{9}{2})$ with the values that are calculated on the assumption of maximal alignment. Namely, in the geometrical picture the magnetic moments of these states can be written as

$$\vec{\mu}(J)=\vec{\mu}_{\mathrm{core}}+\vec{\mu}_F=g_R\vec{I}+g_F\vec{J}_F \tag{12}$$

and therefore

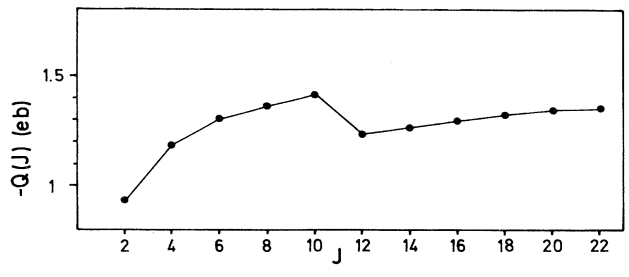

FIG. 3. Electric quadrupole moments of the yrast states from Fig. 1.

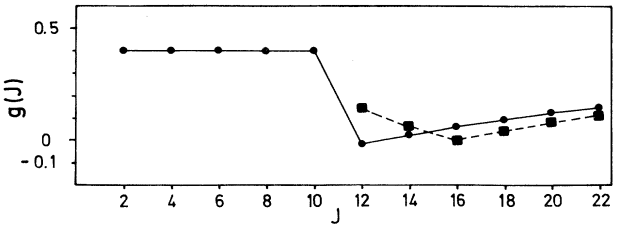

FIG. 4. g factors of the yrast states from Fig. 1 (solid line). The dashed line connects the g factors that are calculated on the assumption of maximal alignment of the unpaired fermions along the axis of rotation [Eq. (14)].

$$g(J)=\frac{1}{J}(g_R^2I^2+g_F^2J_F^2+2g_Rg_F\vec{I}\cdot\vec{J}_F)^{1/2}, \tag{13}$$

where I is the angular momentum of the boson core, J_F is the angular momentum of the unpaired fermions, and J is the total angular momentum. g_R and g_F are the gyromagnetic factors of the boson core and the two-fermion state, respectively. Naturally, neither I nor J_F are exact quantum numbers in the wave functions that are obtained by diagonalization. But, if we assume that in the yrast 2qp band the two fermions are maximally aligned with the axis of rotation, then

$$J_F\simeq(J_F)_{\max}=2j-1\ ,$$

$$\vec{I}\|\vec{J}_F\ ,$$

and

$$I\simeq J-(J_F)_{\max}\ .$$

From (13) we derive the g factors for 2qp states with maximal alignment:

$$g(J)=\frac{1}{J}[g_R^2J^2+(g_R-g_F)^2J_{F\max}^2 -2g_R(g_R-g_F)JJ_{F\max}]^{1/2}\ . \tag{14}$$

In our example the fermions occupy the neutron orbital $h\frac{11}{2}$. Therefore, $J_{F\max}=10$ and $g_F=g_S/2j$ (for $j=l+\frac{1}{2}$). $g_R=0.4$ and, for $g_S=0.7g_S^{\mathrm{free}}$, $g_F=-0.24$. The g factors calculated from Eq. (14) are connected by the dashed line in Fig. 4. The largest difference to the $g(J)$ that are obtained by diagonalization is near the point of crossing, and the states of the yrast 2qp band $(\frac{11}{2},\frac{9}{2})$ become more and more aligned with increasing angular momentum.

We now turn our attention to the effects of the mixing interaction (6) on the electromagnetic properties of yrast states. As we have shown in paper I, the mixing interaction has a very small effect on the yrast states that belong to the 2qp band $(\frac{11}{2},\frac{9}{2})$. On the other hand, the mixing with 2qp states results in an increase of the moment of inertia of the ground-state band and the backbending becomes more pronounced. The percentage of 2qp admixtures in the GSB is proportional to the strength of the mixing interaction. Because of the bending of the GSB, the point of crossing with the band $(\frac{11}{2},\frac{9}{2})$ is shifted to-

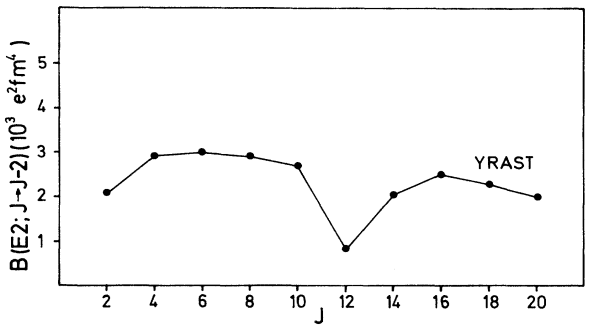

FIG. 5. $B(E2)$ values for transitions between yrast states in the decoupling limit (see Fig. 1). The mixing interaction (6) has been included in the Hamiltonian with $u_2=0.175$ MeV.

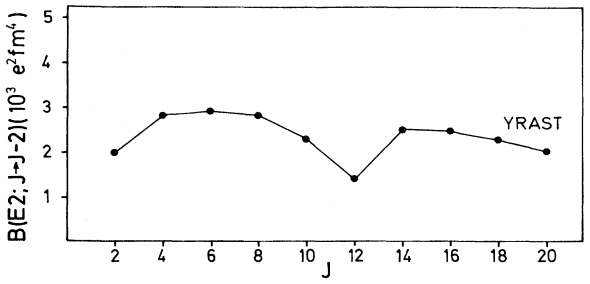

FIG. 6. $B(E2)$ values as in Fig. 5, except that here the strength of the mixing interaction is $u_2=0.275$ MeV.

ward higher angular momenta. In the region above yrast the density of states increases.

In Fig. 5 we present the $B(E2)$ values calculated for transitions between yrast states with inclusion of the mixing interaction (6). In the new parametrization, referred to as parametrization (B), we employ the same set of parameters as in parametrization (A), except that now the mixing interaction (6) has been included in the Hamiltonian with $u_2=0.175$ MeV. The strength of the interaction has been chosen in such a way as to produce the maximum of mixing, retaining at the same time the point of crossing between the two lowest bands between $J=10$ and $J=12$. The amount of 2qp admixtures in the lowest band is presented in Table I. The percentage of 2qp admixtures in the ground-state band is 7% for the ground state $|0_1\rangle$, and increases slowly to 12% for $|10_1\rangle$. The first 2qp yrast state $|12_1\rangle$ has 20% admixtures of pure collective states. The other members of the yrast band $(\frac{11}{2},\frac{9}{2})$ are practically unaffected by the mixing interaction. Because of the mixing between the lowest two bands, the transition $12_1\rightarrow 10_1$ is now relatively strong: $B(E2,\ 12_1\rightarrow 10_1)=0.81\times 10^3\ e^2\text{fm}^4$; an increase of more than five orders of magnitude. In a further step we have increased the mixing interaction to $u_2=0.275$ MeV. In order to retain the point of intersection between $|10_1\rangle$ and $|12_1\rangle$, we have also increased the strength of the dynamical interaction to $\Gamma_0=0.6$ MeV. This parametrization will be referred to as parametrization (C). The 2qp admixtures in the GSB are now more pronounced: from 25% for $|0_1\rangle$ to 33% for $|8_1\rangle$, and almost 50% for $|10_1\rangle$. The state $|12_1\rangle$ has only 3% admixtures of pure collective states. The $B(E2)$'s for transitions between yrast states are shown in Fig. 6. It is seen that the transition between the lowest two bands ($12_1\rightarrow 10_1$) is now comparable to the transitions within the ground-state band. Comparing Figs. 5 and 6 with the $B(E2)$'s that are calculated without mixing interaction (Fig. 2), we note a very interesting result. Although the mixing interaction strongly affects the transitions in the region of band crossing, it produces practically no effect on the transitions within the ground-state band, even when the percentage of 2qp admixtures is rather high (more than 20%). The same is true for the behavior of the quadrupole moments and g factors. In the following section we will discuss this effect in the framework of nuclear Ward identities.

TABLE I. Two-quasiparticle admixtures in the wave functions of the yrast part of the ground-state band. The percentage of 2qp admixtures corresponds to the parametrizations (B) and (C). For a description of parameters, see the text.

States	2qp admixtures (B)	2qp admixtures (C)
0_1	7%	25%
2_1	7%	25%
4_1	8%	27%
6_1	9%	29%
8_1	10%	33%
10_1	12%	50%

III. PARTIAL CANCELLATIONS OF MIXING CONTRIBUTIONS TO TRANSITIONS WITHIN THE GROUND-STATE BAND

We have seen that the two-quasiparticle admixtures in the wave functions of the ground-state band increase with the strength of the mixing interaction. However, this mixing in the wave functions has practically no influence on the $E2$ transition moments. In order to clarify this point we present in Table II the partial contributions to the transition moments $\langle J-2\|T(E2)\|J\rangle$ that are calculated for the parametrization (B). Comparing the last two columns, which give the transition moments for the parametrizations (B) (with the mixing parameter $u_2=0.175$ MeV) and (A) (without mixing), it is obvious that the effect of mixing on $E2$ transitions within the ground-state band is almost negligibly small (less than 0.2%). On the other hand, the influence of mixing in the wave functions is clearly seen in the partial contributions. In the second column we display the partial contributions coming from the purely collective parts of the wave functions (N bosons, 0qp), and in the fourth column the contributions from the blocks in the wave functions that contain 2qp states ($N-1$ bosons, 2qp). The terms in the $E2$

TABLE II. Partial contributions to the transition moments for $E2$ transitions within the yrast part of the ground-state band. In the second, third and fourth columns we present, for the parametrization (B), the partial contributions from matrix elements between the components with (N bosons, 0qp), between the components with (N bosons, 0qp) and ($N-1$ bosons, 2qp), and between the components with ($N-1$ bosons, 2qp), respectively. In the fifth column the total transition moments for the parametrization (B) are displayed. For comparison, in the sixth column we display the reduced matrix elements calculated for the parametrization (A) (without 2qp admixtures). All values are in e fm^2.

$J\rightarrow J-2$	0qp/0qp B	0qp/2qp B	2qp/2qp B	$J/J-2$ B	$J/J-2$ A
$2_1\rightarrow 0_1$	94.5	0.7	6.6	101.8	101.8
$4_1\rightarrow 2_1$	148.9	1.1	10.9	160.9	161.1
$6_1\rightarrow 4_1$	182.0	1.4	14.6	198.0	198.2
$8_1\rightarrow 6_1$	202.7	1.6	18.5	222.8	223.1
$10_1\rightarrow 8_1$	212.0	1.8	23.4	237.2	237.7

operator that do not conserve separately the number of fermions and the number of bosons, give the partial contributions shown in the third column of Table II (0qp–2qp blocks). Comparing the second and the last column in Table II, we see that the mixing interaction reduces the purely collective contribution to the transition moments by 7% (for $2_1\rightarrow 0_1$) to 11% (for $10_1\rightarrow 8_1$). This effect corresponds in magnitude to the reduction of the zero-quasiparticle components in the wave functions of the $0_1, 2_1, \ldots 8_1$ states. However, as seen from Table II, the reduction of the purely collective contribution to the reduced matrix element is practically accounted for by the contributions arising from two-quasiparticle components in the wave functions (third and fourth column). The reduction of the zeroth-order contribution $\langle 0\text{qp}\|T(E2)\|0\text{qp}\rangle$ is obviously due to the renormalization of the corresponding amplitudes in the wave functions. Thus, in the perturbation treatment this reduction is due to the self-energy corrections. In the same approach, the matrix elements that involve 2qp states, $\langle 2\text{qp}\|T(E2)\|2\text{qp}\rangle$, should be associated with vertex corrections. Therefore, the results displayed in Table II can be interpreted in the perturbation approach as evidence that the self-energy and vertex corrections exhibit a tendency towards mutual cancellation. As is well known, a general quantum mechanical feature of cancellation between self-energy and vertex corrections is related to the Ward indentity, which was first formulated in quantum electrodynamics. In quantum electrodynamics the Ward identity expresses the fact that electron self-energy and vertex corrections mutually cancel in the limit of low-momentum transfer which is a consequence of charge conservation [12]. Analogous relations, related to the conservation of the number of particles, appear in the treatment of the many-body problem of the fermion-phonon system in solid-state physics (Ward-Piaterskii identities) [13]. The results of microscopic calculations performed by using the G-matrix for effective nuclear interactions have been also interpreted in a similar framework. Namely, the sets of diagrams which are connected by the conservation of the number of particles [number conserving sets (NCS's)] are predicted to tend to cancel [14]. However, in realistic calculations they cancel rather poorly [15]. In Ref. [16] it was shown that the second- and third-order NCS's for the $E2$ moment exactly cancel in the particle-vibration coupling model in the asymptotic limit of large j. Such a feature was referred to as the nuclear Ward identity. In the realistic case of particle-vibration coupling the tendency towards cancellation of self-energy and vertex corrections is strongly pronounced. This is in agreement with the observation that, although the particle-vibration coupling is not weak, some low-order diagrams often exhibit the main feature of exact solutions obtained by diagonalization. The guideline in selecting such diagrams is to neglect the NCS's consisting of vertex and self-energy corrections. This approach was also applied to the problem of $M1$ moments [17].

Here we extend this approach to a more general situation of boson-fermion systems. In analogy to the previous considerations, diagrams that correspond to a boson-fermion system can be decomposed into dynamical and kinematical parts that enable a transparent treatment of the problem. Similarly as in the particle-vibration model [18], the dynamical contribution can be expressed by Goldstone-type rules and the kinematical part by the corresponding Jucys-Bairdzaites-Vizbanaite (JBV) diagrams of the same topological structure. Let us first consider the system from Sec. II in the absence of mixing between bosons and 2qp states ($u_2=0$). In the SU(3) limit, investigated here, the contributing diagrams can be schematically presented by the diagrams (a), (b) and (c) in Fig. 7. The diagrams (a) and (b) represent the matrix elements $\langle J-2\|e^{\text{vib}}s^\dagger d\|J\rangle=\langle C\|P^\dagger_{J-2}e^{\text{vib}}s^\dagger dP_J\|C\rangle$ and $\langle J-2\|e^{\text{vib}}d^\dagger s\|J\rangle=\langle C\|P^\dagger_{J-2}e^{\text{vib}}d^\dagger sP_J\|C\rangle$, respectively. Here $|C\rangle$ denotes the SU(3) coherent state, and $P_J|C\rangle$ is a state of the ground-state band with angular momentum J projected out of the coherent state [19]. Heavy vertical lines denote the coherent-state boson condensate, and the wavy lines denote the propagation of a d boson (the s boson is included in the reference state for diagrammatic presentation). The dotted horizontal line with $\times$ at the free end represents the $E2$ operator, the strength of which is $e^{\text{vib}}(N-N_d)^{1/2}$ [Figs. 7(a) and 7(b)],

and $\pm e^{\text{vib}}7^{1/2}/2$ [Fig. 7(c)]. The coherent state has a broad d boson number distribution [19], with the maximum at $N_d \approx \frac{2}{3}N$. Only one d boson at a time is interacting with the $E2$ operator, and this one is presented as a relevant partial structure of the coherent state, with other d bosons immersed in the intrinsic state. However, each d boson is symmetrized with other d bosons that are present in the same state.

Let us now discuss the diagrammatic structure in the presence of the mixing interaction (6), which mixes states with different number of quasiparticles. In this case the diagrams (a), (b), and (c) in Fig. 7 are the leading-order diagrams. Additional second-order $\Delta N_d = 1$ self-energy diagrams, deriving their parentage from the diagram in Fig. 7(a), are schematically displayed in Figs. $7(a_1)$–$7(a_6)$. The second-order induced fermion-type diagrams in Fig. $7(a_7)$ and $7(a_8)$, which are due to the second term in the operator (8), have a pattern of vertex corrections associated with self-energy corrections (propagator renormalization). To each fermion-type diagram (a_7), (a_8), there corresponds a class of induced boson-type diagrams, referred to as polarization terms. They give an enhancement of the basic process. The diagrams $(a_{7,1})$–$(a_{7,4})$ in Fig. 7 present the polarization diagrams corresponding to the fermion-type diagram (a_7). We note that the diagrams (a_1)–(a_3), (a_7), and $(a_{7,1})$–$(a_{7,4})$ correspond to the NCS. Considering an analogy to Ref. [16] in the asymptotic limit of large j, it follows that the sign of the vertex corrections (a_7), $(a_{7,1})$–$(a_{7,4})$ is opposite to that of the self-energy corrections (a_1)–(a_3). The propagator renormalization in the diagrams (a_1)–(a_3) gives a contribution with negative sign (representing renormalization due to creation of two-quasiparticle pairs), while the vertex corrections in (a_7), $(a_{7,1})$–$(a_{7,4})$ involve a recoupling term with

$$(-1)\langle j \| Y_2 \| j \rangle \begin{Bmatrix} 2 & 2 & 2 \\ j & j & j \end{Bmatrix},$$

which is a positive quantity. In analogy to the previous considerations, all diagrams, except the leading-order (a), (b), and (c), tend to cancel in the asymptotic limit. In other words, a decrease of the transition moment due to normalization tends to be compensated by vertex corrections; the total result being close to the zeroth-order term (i.e. without the 2qp admixtures). We note that the normalization corrections represent a renormalization of the bare matrix elements due to the reduction of the main components in the wave functions. The probability that bosons will interact with the external electromagnetic field, without a cloud of virtual two-fermion states, is no longer unity. It is reduced by the probability of having virtual two-fermion states associated with d bosons. The approximate cancellation of the propagator renormalization and vertex correction is clearly reflected in the results presented in Table II for transitions within the ground-state band.

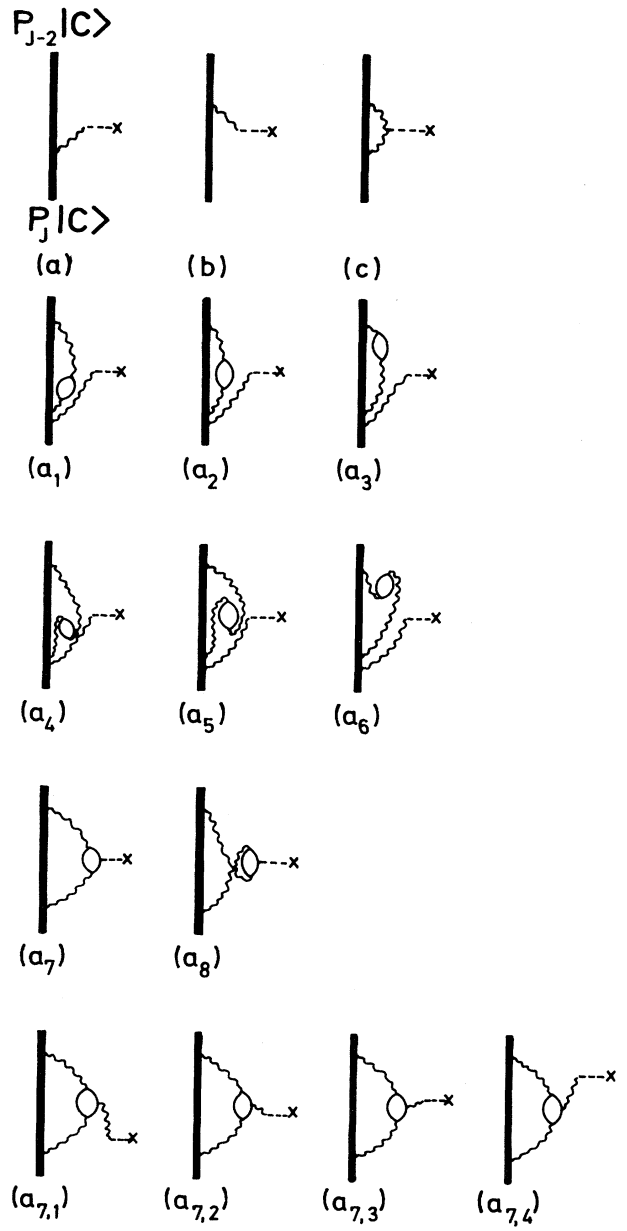

FIG. 7. Some classes of low-order diagrams for $E2$ transition moments involving mixing of boson and two-quasiparticle states.

IV. STRONG COUPLING

Our second example treats the case of two hole-type (particle-type) fermions coupled to the SU(3) prolate (oblate) core. The analog situation in the geometrical model [9] arises for the case of strong coupling of two unpaired fermions to the deformation. In Fig. 8 we present the energy spectrum that is obtained by diagonalization of the Hamiltonian (1) in the basis (7), for the same set of parameters as in the first example from Sec. II, except that now $v^2 = 0.8$ and $\Gamma_0 = 0.39$ MeV. The mixing interaction (6) is not included in the calculation. The un-

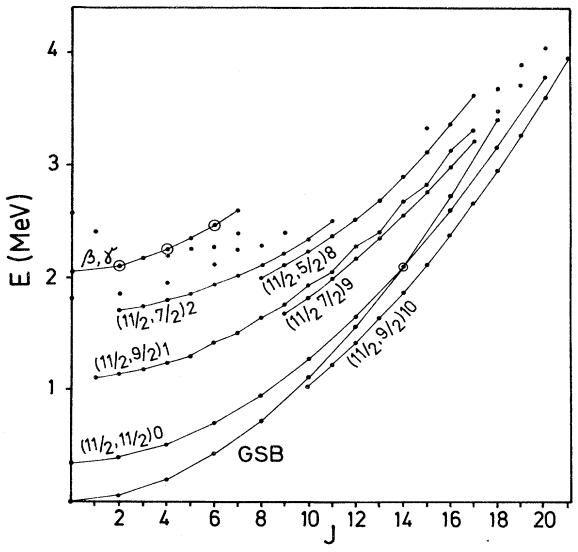

FIG. 8. The energy spectrum that is calculated for the same set of parameters as the one shown in Fig. 1, except that here $v^2=0.8$ and $\Gamma_0=0.39$ MeV.

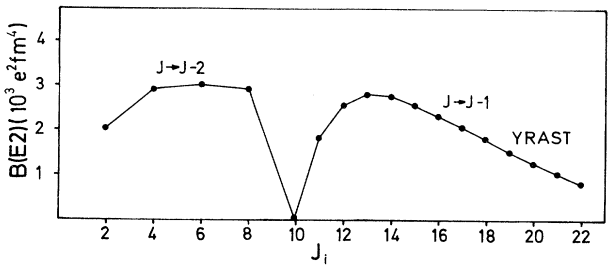

FIG. 9. $B(E2)$ values for transitions between the yrast states from Fig. 8. In the 2qp band $(\frac{11}{2},\frac{9}{2})10$ the transition probabilities correspond to $\Delta J=1$ transitions.

paired fermions have been changed from particlelike to holelike, and therefore the dynamical interaction becomes attractive (the core is prolate). The spectrum presents a strongly coupled band pattern. The low-lying 2qp states are organized into $\Delta J=1$ rotational bands. These bands are, apart from Coriolis effects, described by the algebraic K quantum numbers $(K_1,K_2)K$ (Refs. [7,11]). In analogy to the case [20,21] of one fermion coupled to the SU(3) core, in the geometrical limit $N\rightarrow\infty$ the algebraic quantum numbers K_1, K_2, and K correspond to the projections on the symmetry axis of the angular momenta j_1 and j_2, and the total angular momentum J, respectively. In our example $j_1=j_2=\frac{11}{2}$. The lowest bands have the highest values of K_1 and K_2. At angular momentum $J=10$ the 2qp band $(\frac{11}{2},\frac{9}{2})10$ becomes the yrast band. This band has $K=10$ and the GSB has $K=0$. Therefore, with the inclusion of the mixing interaction (6), which is of rank 2 in the fermion part, the band $(\frac{11}{2},\frac{9}{2})10$ practically will not mix with the ground-state band. Including the mixing interaction, the main contributions to 2qp admixtures in the ground-state band come from the bands $(\frac{11}{2},\frac{11}{2})0$ and $(\frac{11}{2},\frac{9}{2})1$. Since $K=0$, the $(\frac{11}{2},\frac{11}{2})0$ band contains only even-spin states. In the $(\frac{11}{2},\frac{9}{2})1$ band we notice the odd-even staggering for high-spin states, which is caused by the interacting boson-fermion model (IBFM) analog [22,23] of the Coriolis interaction. As in the limit of decoupling, states high above the yrast line show much more mixing, and it is practically impossible to identify rotational bands.

The $B(E2)$ values for transitions between the yrast states are shown in Fig. 9. Up to $J=8$ the transitions are within the ground-state band. There is practically no transition between the band $(\frac{11}{2},\frac{9}{2})10$ and the GSB, i.e. $B(E2;\ 10_1\rightarrow 8_1)\approx 0$. Above $J=10$ the $B(E2)$'s correspond to $\Delta J=1$ transitions within the band $(\frac{11}{2},\frac{9}{2})10$. The $B(E2)$ values for $\Delta J=2$ transitions within the yrast band $(\frac{11}{2},\frac{9}{2})10$ are displayed in Fig. 10, in comparison with transition probabilities for the ground-state band. In Fig. 10 we have also included the $B(E2)$'s for transitions within the 2qp band $(\frac{11}{2},\frac{11}{2})0$. It is seen that, although somewhat lower (i.e., there is less collectivity), these probabilities follow closely the behavior of $B(E2)$'s for transitions within the GSB. The quadrupole moments of the yrast states are given in Fig. 11. Note the sharp change in sign between $J=8_1$ and $J=10_1$, as the 2qp band $(\frac{11}{2},\frac{9}{2})10$ becomes the yrast band. Finally, in Fig. 12 we display the g factors of yrast states. In the GSB they have the constant value $g_R=0.4$. There is a change in sign in passing to the 2qp band $(\frac{11}{2},\frac{9}{2})10$, and then a steady increase with increasing angular momentum. At $J=13$ the g factor is again positive.

The inclusion of the mixing interaction (6) in the Hamiltonian will give rise to 2qp admixtures in the GSB and therefore to an increase of the moment of inertia [7]. In analogy to the decoupled case (Secs. II and III), for a realistic strength (5–30% 2qp admixtures in the wave functions), the mixing interaction does not change the electromagnetic properties of states of the GSB. We have also explained that the mixing interaction (fermion rank

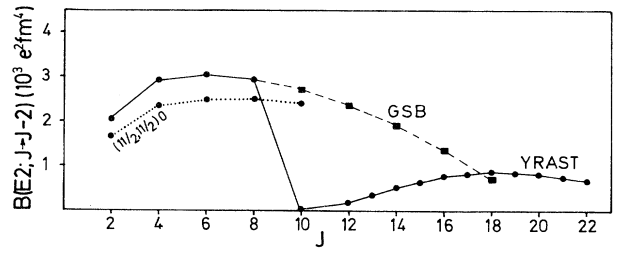

FIG. 10. $B(E2)$ values for transitions in the limit of strong coupling (Fig. 8): $\Delta J=2$ transitions between the yrast states (solid line), transitions within the ground-state band (dashed line), and transitions within the band $(\frac{11}{2},\frac{11}{2})0$ (dotted line).

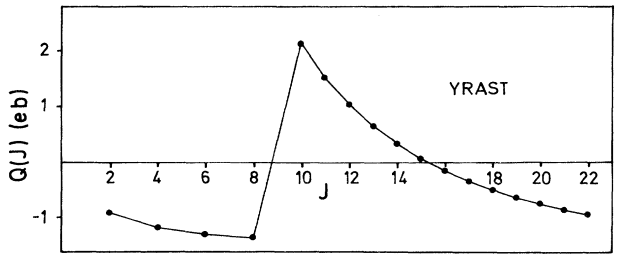

FIG. 11. Electric quadrupole moments of the yrast states from Fig. 8.

2), has no effect on the 2qp yrast band $(\frac{11}{2},\frac{9}{2})10$. In the limit of decoupling (Sec. II), we have seen how the mixing interaction affects the transitions in the region of crossing between the GSB and the lowest 2qp band. Even for a moderately strong interaction, the transition between the two bands increases by several orders of magnitude and becomes comparable to collective transitions in the GSB. In the limit of strong coupling, however, this is not the case. The transitions between the $(\frac{11}{2},\frac{9}{2})10$ band and the ground-state band are $\Delta K=10$ forbidden. Even for a very strong mixing interaction these transitions are negligible. Let us now return for a moment to the strong-coupling spectrum in Fig. 8. A very interesting question is whether the mixing between the two lowest $K=0$ bands, the ground-state band and the $(\frac{11}{2},\frac{11}{2})0$ band, will also give rise to significant $\Delta J=0$ transitions between the two bands. The answer is no. We have recalculated the strong-coupling spectrum, but now including the mixing interaction (6) with $u_2=0.09$ MeV. The band $(\frac{11}{2},\frac{9}{2})10$ crosses the GSB between $J=10$ and $J=12$. The percentage of 2qp admixtures in the yrast part of the GSB goes from 17% for $|0_1\rangle$ to 25% for $|10_1\rangle$. If we consider the $\Delta J=0$ transitions between the $(\frac{11}{2},\frac{11}{2})0$ band and the GSB, we note that systematically the partial contributions to the reduced matrix elements that come from the purely collective parts of the wave functions ($|N$bosons$\rangle$), are almost identical in magnitude, but opposite in sign, to the contributions from the blocks in the wave functions that contain 2qp states ($|(N-1)$ bosons$\otimes$2qp$\rangle$). The resulting reduced matrix elements are all small. Consider, for example, the transition $(\frac{11}{2},\frac{11}{2})0J=6_2\rightarrow 6_1$. The contribution to the reduced matrix element that comes from the purely collective part is 71.6 e fm^2, the contribution from the $(N-1)$bosons$\otimes$2qp block is -64.1 e fm^2, and the contribution from the 0qp–2qp block is -0.91 e fm^2. The resulting $B(E2)$ is 3.3 e^2fm^4. We compare this value to the transition within the band: $B(E2;(\frac{11}{2},\frac{11}{2})0\,J=6_2\rightarrow(\frac{11}{2},\frac{11}{2})0\,J=4_2)=2532$ e^2fm^4, with partial contributions to the reduced matrix element: 35.6 e fm^2 from the purely collective part, 147.5 e fm^2 from the $(N-1)$ bosons $\otimes$2qp block, and -1.63 e fm^2 from the 0qp–2qp block. This effect is observed for all states of the $(\frac{11}{2},\frac{11}{2})0$ band. Thus, although $\Delta K=0$, the $\Delta J=0$ transitions between the $(\frac{11}{2},\frac{11}{2})0$ band and the ground-state band are all of the order of 1 e^2fm^4, three orders of magnitude weaker than the corresponding $\Delta J=2$ interband transitions.

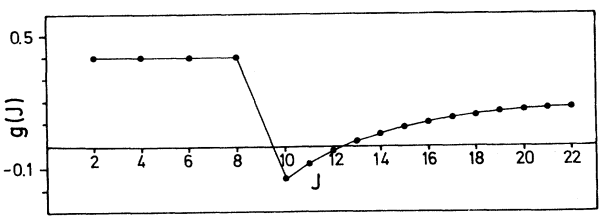

FIG. 12. g factors of the yrast states from Fig. 8.

V. CONCLUSIONS

In this work we have investigated the electromagnetic properties of yrast states in the SU(3) limit of the IBA model extended by the inclusion of two-quasiparticle states. In the previous publication [7] we have investigated the formation of band patterns based on two- and four-quasiparticle excitations out of the boson space. In particular, we have shown that for particle-type (hole-type) fermions coupled to the SU(3) prolate (oblate) IBM core, a new algebraic decoupling basis arises for the lowest two-quasiparticle bands (in analogy to Stephens' rotation aligned basis). For hole-type (particle-type) fermions coupled to the SU(3) prolate (oblate) core we have derived the algebraic K-representation basis which describes the low-lying 2qp bands (in analogy to the strong-coupling basis of the Bohr-Mottelson model). In the present paper we have performed an illustrative calculation of electromagnetic properties of yrast states for these limiting cases of coupling two-quasiparticle states to the SU(3) boson core. In the decoupling limit, we have shown that the pair-breaking interaction, which mixes states with different number of quasiparticles, has strong influence on transitions in the region of crossing between the ground-state band and the lowest two-quasiparticle band ($\alpha_1=j$, $\alpha_2=j-1$). Even for a rather weak interaction, the transition between the two bands is comparable in strength to the collective interband transitions. On the other hand, the influence of the mixing interaction on transitions within the ground-state band below the point of intersection is very small. This effect appears in spite of sizeable 2qp admixtures in the corresponding wave functions and is due to the approximate cancellation of the self-energy and vertex corrections, which is an analog of the nuclear Ward identity. We obtain similar results for the behavior of static electric quadrupole and magnetic dipole moments.

In the strong-coupling limit the two-quasiparticle states are organized into $\Delta J=1$ bands, and are described by the algebraic K quantum numbers $(K_1,K_2)K$, with the lowest two-quasiparticle band being $(K_1=j,$ $K_2=j-1)K=2j-1$. Thus, the transitions between the

lowest two-quasiparticle band and the ground-state band are highly forbidden ($\Delta K = 2j - 1$). The mixing interaction, which is of rank 2 in the fermion part, has practically no effect on these transitions. The mixing between the two lowest $K = 0$ bands, the ground-state band and the $(j,j)0$ band, is sizeable, but the influence on $\Delta J = 0$ $E2$ transitions between these bands is small because of incoherence between partial contributions.

[1] F. Iachello and A. Arima, *The Interacting Boson Model* (Cambridge University Press, Cambridge, England, 1987).
[2] A. Gelberg and A. Zemel, Phys. Rev. C **22**, 937 (1980).
[3] I. Morrison, A. Faessler, and C. Lima, Nucl. Phys. **A372**, 13 (1981); S. Kuyucak, A. Faessler, and M. Wakai, *ibid.* **A420**, 83 (1984); A. Faessler, S. Kuyucak, A. Petrovici, and L. Petersen, *ibid.* **A438**, 78 (1985).
[4] N. Yoshida, A. Arima, and T. Otsuka, Phys. Lett. **114B**, 86 (1982); N. Yoshida and A. Arima, *ibid.* **164B**, 231 (1985).
[5] C. E. Alonso, J. M. Arias, and M. Lozano, Phys. Lett. B **177**, 130 (1986).
[6] D. S. Chuu and S. T. Hsieh, Phys. Rev. C **38**, 960 (1988); D. S. Chuu, S. T. Hsieh, and H. C. Chiang, *ibid.* C **40**, 382 (1989).
[7] D. Vretenar, V. Paar, G. Bonsignori, and M. Savoia, Phys. Rev. C **42**, 993 (1990).
[8] F. Iachello and D. Vretenar, Phys. Rev. C **43**, 945 (1991).
[9] A. Bohr and B. R. Mottelson, *Nuclear Structure* (Benjamin, New York, 1975).
[10] F. S. Stephens, Rev. Mod. Phys. **47**, 43 (1975).
[11] D. Vretenar, S. Brant, V. Paar, and D. K. Sunko, Phys. Rev. C **41**, 757 (1990).
[12] S. S. Schweber, *An Introduction to Relativistic Quantum Field Theory* (Row, Peterson and Co., New York, 1961).
[13] P. Nozières, *Theory of Interacting Fermi Systems* (Benjamin, New York, 1964).
[14] B. Brandow, in *Quantum Fluids and Nuclear Matter,* Lectures in Theoretical Physics, edited by K. T. Mahanthappa and W. E. Brittin (Gordon and Breach, New York, 1969), Vol. XI B, p.55.
[15] B. R. Barret and M. W. Kirson, in *Advances in Nuclear Physics,* edited by M. Baranger and E. Vogt (Plenum, New York, 1973), Vol. VI, p. 219.
[16] V. Paar, Phys. Lett. **60B**, 232 (1975).
[17] V. Paar and S. Brant, Phys. Lett. **74B**, 297 (1978); Nucl. Phys. **A303**, 96 (1978).
[18] V. Paar, Nucl. Phys. **A164**, 576 (1971).
[19] L. F. Canto and V. Paar, Phys. Lett. **102B**, 217 (1981).
[20] O. Scholten, Ph.D. thesis, University of Groningen, 1980.
[21] O. Scholten, Prog. Part. Nucl. Phys. **14**, 189 (1985).
[22] A. Arima, A. Gelberg, and O. Scholten, Phys. Lett. **185B**, 259 (1987).
[23] D. K. Sunko and V. Paar, Phys. Lett. **199B**, 482 (1987).